Chapter 6
Three-Dimensional Hamiltonian Problems

In the present chapter, we broaden the quantum mechanical treatment of the problem of a single particle moving in three-dimensional space to incorporate the Hamiltonian. We only treat central potentials $V(\boldsymbol{r}) = V(r)$. In particular, we study the Coulomb and the three-dimensional harmonic oscillator potentials, including Rydberg atoms. We also present the spin–orbit interaction and elements of scattering theory.

6.1 Central Potentials

The solution to a given problem can be simplified by exploiting the associated symmetries. We have already shown that this is the case by applying invariance under the inversion operation (see the bound problems of Sects. 4.2 and 4.4). Since problems involving a central potential $V(r)$ are spherically symmetric, we shall make use of this symmetry. For this purpose, we write the kinetic energy Laplacian in spherical coordinates (5.10). The total Hamiltonian reads

$$\begin{aligned}\hat{H} &= \frac{1}{2M}\left(\hat{p}_x^2 + \hat{p}_y^2 + \hat{p}_z^2\right) + V(r)\\ &= \frac{\hbar^2}{2M}\left(-\frac{\partial^2}{\partial r^2} - \frac{2}{r}\frac{\partial}{\partial r}\right) + \frac{\hat{L}^2}{2Mr^2} + V(r),\end{aligned} \tag{6.1}$$

where the operator $\hat{L}^2$ is the square of the orbital angular momentum (5.11). Since the Hamiltonian (6.1) commutes with operators $\hat{L}^2$ and $\hat{L}_z$, there is a basis set of eigenfunctions for the three operators. The eigenvalue equation (4.11) is solved by factorizing the wave function into radial and angular terms, the latter being represented by the spherical harmonics (5.62):

$$\Psi(r, \theta, \phi) = R_{n_r l}(r) Y_{l m_l}(\theta, \phi). \tag{6.2}$$

D. Bes, *Quantum Mechanics*, Graduate Texts in Physics,
DOI 10.1007/978-3-642-20556-9_6,

In such a case, the operator $\hat{L}^2$ in the kinetic energy can be replaced by its eigenvalue $\hbar^2 l(l+1)$, and moreover, the spherical harmonics cancel on both sides of the Schrödinger equation.[1] One is left with a differential equation depending on a single variable: the radius. Thus,

$$\left\{ \frac{\hbar^2}{2M} \left[-\frac{d^2}{dr^2} - \frac{2}{r}\frac{d}{dr} + \frac{l(l+1)}{r^2} \right] + V(r) \right\} R_{n_r l}(r) = E_{n_r l} R_{n_r l}(r), \tag{6.3}$$

where the new quantum number n_r distinguishes between states with the same value of l. Since the magnetic quantum number m_l does not appear in this equation, the eigenvalues $E_{n_r l}$ are also independent of it. In consequence, the eigenenergies of a central potential are necessarily degenerate, with degeneracy equal to $2l+1$ (5.13). This result is to be expected since the quantum number m_l depends on the orientation of the coordinate axis. That is to say, the central potential has spherical symmetry and the resulting energies (which are physical quantities) should not depend on the orientation of the coordinate axis (which is an artifact of the calculation).

Systems for which the number of quantum numbers equals the number of degrees of freedom are called *integrable*. Do not get a wrong impression out of the present chapter: they are the exceptions.

6.1.1 Coulomb and Harmonic Oscillator Potentials

In this section, we discuss the solutions to the eigenvalue equation for two central potentials: the Coulomb potential $-Ze^2/4\pi\epsilon_0 r$ and the three-dimensional harmonic oscillator potential $M\omega^2 r^2/2$.

It is always useful to begin by estimating the orders of magnitude of the quantities involved. For the linear harmonic oscillator, this has already been done in (3.28). These orders of magnitude remain valid for the three-dimensional case, since the harmonic Hamiltonian is separable into three Cartesian coordinates, and the estimate (3.28) holds for each coordinate. For the Coulomb potential, we may again use the Heisenberg uncertainty relations

$$\boldsymbol{p}^2 \approx 3\,(\Delta p_x)^2 \geq \frac{3\hbar^2}{4}\frac{1}{(\Delta x)^2} \approx \frac{9\hbar^2}{4}\frac{1}{r^2}. \tag{6.4}$$

Therefore, the radius r_m is obtained by minimizing the lower bound energy

$$E \geq \frac{9\hbar^2}{8Mr^2} - \frac{Ze^2}{4\pi\epsilon_0 r}, \tag{6.5}$$

[1] This is another application of the separation of variables method for solving partial differential equations.

Table 6.1 Solutions to the Coulomb and harmonic oscillator potentials

Problem	Coulomb	Harmonic oscillator
Characteristic length	$a_0 = 4\pi\epsilon_0\hbar^2/Me^2$	$x_c = \sqrt{\hbar/M\omega}$
Wave function	$R_{n_r l}(u)Y_{lm_l}(\theta,\phi)$ $u = Zr/a_0$	$R_{n_r l}(u)Y_{lm_l}(\theta,\phi)$ $u = r/x_c$
Radial quantum numbers	$n_r = 0, 1, \ldots$	$n_r = 0, 1, \ldots$
Principal quantum numbers	$n = n_r + l + 1 = 1, 2, \ldots$	$N = 2n_r + l$=0,1, ...
Energies	$Z^2 E_H/n^2$ $E_H = -e^2/8\pi\epsilon_0 a_0$	$\hbar\omega(N + 3/2)$
Degeneracy	n^2	$(N + 1)(N + 2)/2$

which yields

$$r_m = \frac{9}{4Z}a_0, \qquad E \geq \frac{16Z^2}{9}E_H, \tag{6.6}$$

where the Bohr radius a_0 and the ground state energy of the hydrogen atom E_H are given in Tables 6.1 and A.1.

The solutions of the Schrödinger equation for the Coulomb[2] and the harmonic oscillator potentials are shown in Table 6.1. The corresponding details are outlined in Sect. 6.4*. The following comments stem from the comparison between the solutions for these two potentials:

- In both cases, the radial factor $R_{n_r l}(r)$ may be expressed as a product of an exponential decay, a power of u, u^l, and a polynomial of degree n_r (Coulomb) or $2n_r$ (harmonic oscillator).
- The radial factor u^l decreases the radial density $|R_{n_r l}|^2 r^2$ for small values of u and increases it for large values. It is a manifestation of centrifugal effects due to rotation of the particle.
- Both potentials display a higher degree of degeneracy than is required by spherical invariance.
- All degenerate states in the harmonic oscillator potential have the same value of $(-1)^l = (-1)^N$, where N is the principal quantum number (Table 6.1) and thus have the same parity. This is not true for the Coulomb potential, where states with even and odd values of l may be degenerate [see the last equation of (5.12)].
- The energies of the Coulomb potential are represented in Fig. 6.1, while those of the harmonic potential have the same pattern as in Fig. 3.2. The eigenvalues of the former display an accumulation point at $E_\infty = 0$. They are equidistant in the harmonic oscillator case.

[2] Solutions for the Coulomb potential applying matrix algebra can be found in [39].

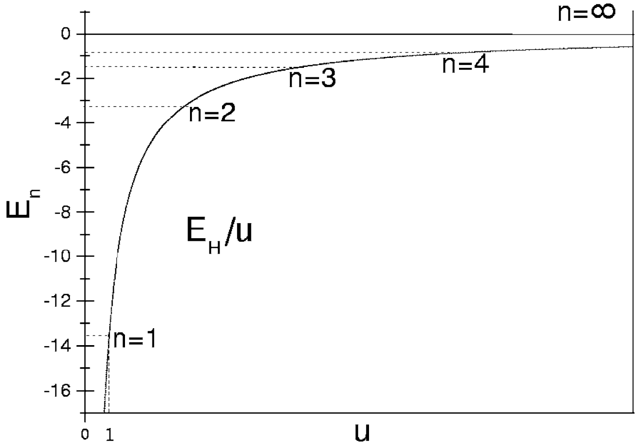

Fig. 6.1 Coulomb potential and its eigenvalues. The dimensionless variable $u = r/a_0$ has been used

We have verified the commonly made statement that the Schrödinger equation is exactly soluble for the two central potentials treated in this section. In fact the two Schrödinger equations are related by a simple change of independent variable $r \to r^2$, if the energy and the strength of the potential are swapped and the orbital angular momentum is rescaled (Problem 8) [40]. Thus, the Schrödinger equations corresponding to the Coulomb and three-dimensional harmonic oscillator potential constitute only one soluble quantum mechanical central problem, not two.

The harmonic oscillator potential is also separable in Cartesian coordinates. As an exercise, derive the degeneracies using the Cartesian solution and check the results against those appearing in the last column of Table 6.1.

While the Coulomb potential is an essential tool for the systematic description of atomic spectra, the three-dimensional harmonic oscillator plays a similar role for the nuclear spectra. This similitude is remarkable in view of the very different constituents and interactions that are present in both systems (Sect. 7.3).

6.1.2 Rydberg Atoms

The set of degenerate single particle levels constitutes a shell (Sect. 7.3). Since all the magnetic substates are filled up in a closed shell, this system displays spherical symmetry. Alkali atoms have one electron outside closed shells. Their spectrum shows to a large extent the characteristic features of single-particle motion, the effect of the closed shell electrons being almost totally limited to screen the nuclear charge. Rydberg atoms are alkali atoms excited to states with large quantum number $n = \mathcal{O}(50)$, carrying an orbital angular momentum $l = n - 1$ with projection $m_l = l$.

Assuming that the outside electron feels a Coulomb potential with charge 1, the energies and wave functions [(6.2) and (6.27)] are given by

$$E_n = -R_H \hbar c/n^2,$$
$$\varphi_{n,n-1,n-1} = \frac{1}{\sqrt{\pi a_0^3}} \frac{1}{n^n n!} \left[-\frac{r}{a_0} \sin\theta \exp(i\phi) \right]^{n-1} \exp(-r/na_0), \tag{6.7}$$

where R_H is approximately the Rydberg constant and a_0 is the Bohr radius (Table A.1).

The mean value of the radius is

$$r_n \equiv \langle n, n-1, n-1|r|n, n-1, n-1\rangle = a_0\, n(2n+1)/2 \approx a_0 n^2, \tag{6.8}$$

which tell us that the radius of the orbit n is much larger than the radius of the core, and that the approximation gets better the higher the value of n. Moreover, the relative dispersion is

$$\frac{\Delta r_n}{r_n} = 1/\sqrt{2n+1}, \tag{6.9}$$

with a similar expression for the θ degree of freedom. Thus the density distribution resembles a tire. In fact, it is the closest that one can get to the circular orbits of the old Bohr atomic model (see Problem 14). The azimuthal angle ϕ is completely unspecified, as required by Heisenberg's uncertainty principle. See also Problem 14 and Problem 14 in Chap. 9.

The coupling with other degenerate states (such as $\varphi_{n,n-2,n-2}$) can become sufficiently small by making use of an electric field along the direction of the angular momentum (Stark effect), which destroys this degeneracy (see Problem 12, Chap. 8).

Rydberg atoms with $40 < n < 60$ are presently used to verify quantum mechanical properties that were discussed by means of thought experiments during most of the last century (Sect. 12.3.3). They are also candidates to play the role of qubits in future quantum computers (Sect. 13.4†).

6.2 Spin–Orbit Interaction

One may incorporate the spin degree of freedom into the present treatment. The degeneracies displayed in Table 6.1 are thus doubled.

According to the results of Sect. 5.3.1, there are two complete sets of wave functions that may take care of the spin $s = 1/2$:

$$\varphi_{nlm_lsm_s} = R_{n_rl} Y_{lm_l} \varphi_{sm_s}, \tag{6.10}$$

$$\varphi_{nlsjm} = R_{n_r l} \sum_{m_l + m_s = m} c(lm_l; sm_s; jm) Y_{lm_l} \varphi_{sm_s}, \tag{6.11}$$

where the Clebsch–Gordan or Wigner coefficients are given in Sect. 5.6*. As mentioned in Sect. 5.3.1, the first set is labeled with the quantum numbers $lm_l sm_s$ specifying the modulus and the z-projection of the orbital angular momentum and the spin. In the second set, the moduli of the orbital angular momentum and the spin remain as good quantum numbers, to be accompanied by jm, associated with the modulus and z-projection of the total angular momentum $\hat{\boldsymbol{J}} = \hat{\boldsymbol{L}} + \hat{\boldsymbol{S}}$.

The Coulomb interaction is the strongest force acting inside an atom, and yields adequate results for many purposes. However, the experimental spectrum displays small shifts in energy associated with values of j. Another (weaker) force that is present in the atom is provided by the interaction between the magnetic moment of the spin and the magnetic field produced by the orbital motion of the electron[3]:

$$\hat{V}_{\rm so} = v_{\rm so} \hat{\boldsymbol{S}} \cdot \hat{\boldsymbol{L}}, \tag{6.12}$$

where we have approximated the radial factor by a constant $v_{\rm so}$.

Suppose we sit on the electron. We see the charged nucleus orbiting around us. The current associated with this moving charged nucleus produces a magnetic field at the location of the electron. The $\hat{\boldsymbol{S}} \cdot \hat{\boldsymbol{L}}$ term can be interpreted as the interaction between the spin magnetic moment of the electron and this magnetic field.

There are additional terms, the hyperfine interactions, arising from the interaction between the nuclear and the electron spins. Although they are even smaller, they produce a splitting of the ground state of the hydrogen atom with astrophysical importance [which the interaction (6.12) does not].

The radial term $R_{n_r l}$ has been dropped in the present section, since the spin–orbit interaction (6.12) does not affect the radial part of the wave function.

The spin–orbit interaction satisfies the commutation relations

$$[\hat{V}_{\rm so}, \hat{L}^2] = [\hat{V}_{\rm so}, \hat{S}^2] = [\hat{V}_{\rm so}, \hat{J}^2] = [\hat{V}_{\rm so}, \hat{J}_z] = 0, \tag{6.13}$$

while $[\hat{V}_{\rm so}, \hat{L}_z] \neq 0$, $[\hat{V}_{\rm so}, \hat{S}_z] \neq 0$. Bearing in mind this property, different procedures – already developed in these notes – may be applied to incorporate the interaction (6.12).

1. The interaction is not diagonal within the set of eigenstates of the projections of the angular momenta (6.10). Since $\hat{V}_{\rm so}$ commutes with $\hat{J}_z$, the spin–orbit interaction conserves the total projection $m = m_l + m_s$ and thus gives rise to matrices of order 2 which may be diagonalized according to Sect. 3.2.

[3] Criteria which are frequently used to construct interactions involving pure quantum variables are (1) simplicity and (2) invariance under transformations, such as rotations, parity and time-reversal operations. The interaction (6.12) satisfies all these criteria. Moreover, it may also be obtained in the non-relativistic limit of the Dirac equation.

2. The spin–orbit interaction is diagonal within the set of eigenstates (6.11). This constitutes a significant advantage. The diagonal matrix elements are the eigenvalues, which may be obtained through calculation.
3. Observing that

$$\hat{\boldsymbol{L}}\cdot\hat{\boldsymbol{S}} = \frac{1}{2}\left(\hat{J}^2 - \hat{L}^2 - \hat{S}^2\right), \tag{6.14}$$

we obtain

$$\langle lsjm|\boldsymbol{S}\cdot\boldsymbol{L}|lsjm\rangle = \frac{\hbar^2}{2}\left[j(j+1) - l(l+1) - \frac{3}{4}\right]. \tag{6.15}$$

Due to the spin–orbit interaction, the two states with $j_\pm = l \pm 1/2$ become displaced by an amount proportional to the values appearing on the right-hand side of (6.15).

6.3 Some Elements of Scattering Theory

6.3.1 *Boundary Conditions*

We consider an incident particle scattered by a central, finite-sized potential. The asymptotic boundary condition for this problem requires the asymptotic wave function to be expressed as a superposition of an incident plane wave along the z-axis and an outgoing spherical wave (Fig. 6.2):

$$\lim_{r\to\infty} \Psi(r,\theta) = A\left[\exp(\mathrm{i}kz) + \frac{\exp(\mathrm{i}kr)}{r} f_k(\theta)\right], \tag{6.16}$$

where $k = \sqrt{2ME}/\hbar$ is the wave number (4.32) and $f_k(\theta)$ is the amplitude of the scattered wave in the polar direction θ. The spherical wave carries a factor $1/r$, since

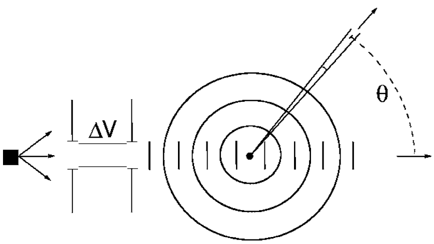

Fig. 6.2 Schematic representation of a scattering experiment. After being produced in a source, the projectile is collimated, accelerated and collimated again. It collides with the target in the form of a plane wave. It is subsequently scattered as a spherical wave, within a solid angle that makes an angle θ with the direction of incidence

$|\Psi(r)|^2$ must be proportional to $1/r^2$ to conserve probability (see Problem 11). The azimuth angle ϕ does not appear, because the problem displays axial symmetry. Expression (6.16) constitutes a generalization of the boundary conditions discussed at the beginning of Sect. 4.5 to the three-dimensional case.

6.3.2 Expansion in Partial Waves

As in the case of a three-dimensional harmonic oscillator, the free particle problem admits solutions in both Cartesian and polar coordinates. The solutions to the Hamiltonian (6.1) with $V(r) = 0$ are, in spherical coordinates,

$$\varphi^{(1)}_{lm_l}(r,\theta,\phi) = j_l(kr)Y_{lm_l}(\theta,\phi), \qquad \varphi^{(2)}_{lm_l}(r,\theta,\phi) = n_l(kr)Y_{lm_l}(\theta,\phi), \quad (6.17)$$

where j_l and n_l are Bessel and Neumann functions, respectively (see Sect. 6.5*). The eigenstates (6.17) constitute a complete set. Our immediate task is to construct the most general linear combination which asymptotically yields (6.16). We first note that the function $\exp(\mathrm{i}kz)$ may be expanded as

$$\exp(\mathrm{i}kz) = \sqrt{4\pi}\sum_{l=0}^{l=\infty} \mathrm{i}^l(2l+1)^{1/2} j_l Y_{l0}. \quad (6.18)$$

Secondly, the second term on the right-hand side of (6.16) can be written in terms of the Hankel function of the first kind, which behaves asymptotically as an outgoing spherical wave (6.37). Therefore, the most general and acceptable linear combination is

$$\begin{aligned}\Psi(r,\theta) &= A\sum_{l=0}^{l=\infty}\left[\sqrt{4\pi}\mathrm{i}^l(2l+1)^{1/2}j_l + c_l h_l^{(+)}(kr)\right]Y_{l0} \\ &= A\sqrt{\pi}\sum_{l=0}^{l=\infty}\mathrm{i}^l(2l+1)^{1/2}a_l\left(j_l\cos\delta_l - n_l\sin\delta_l\right)Y_{l0}. \quad (6.19)\end{aligned}$$

Here c_l, a_l are complex amplitudes, which may be expressed in terms of δ_l, the (real) phase shift of the l-partial wave:

$$c_l = \sqrt{\pi}\mathrm{i}^l(2l+1)^{1/2}(a_l^2 - 1), \qquad a_l = \exp(\mathrm{i}\delta_l). \quad (6.20)$$

We notice that $f_k(\theta)$ is provided by the second term in the first line of (6.19). Replacing the Hankel function by its asymptotic representation one gets

$$f_k(\theta) = -\mathrm{i}\frac{\sqrt{\pi}}{k}\sum_{l=0}^{l=\infty}(2l+1)^{1/2}\left[\exp(\mathrm{i}2\delta_l) - 1\right]Y_{l0}. \quad (6.21)$$

6.3.3 Cross Sections

According to (6.16), the ratio between the scattered flux in the direction θ and the incident flux along the polar axis is given by $|f(\theta)|^2/r^2$. The differential cross section is defined as the number of particles that emerge per unit incident flux, per unit solid angle and per unit time:

$$\sigma(\theta) = |f(\theta)|^2 = \frac{\pi}{k^2}\left|\sum_{l=0}^{l=\infty}(2l+1)^{1/2}\big[\exp(\mathrm{i}2\delta_l) - 1\big]Y_{l0}\right|^2. \tag{6.22}$$

The total cross section is the integral over the whole solid angle

$$\sigma = 2\pi\int_0^\pi \sigma(\theta)\sin\theta \mathrm{d}\theta = \frac{4\pi}{k^2}\sum_{l=0}^{l=\infty}(2l+1)\sin^2\delta_l. \tag{6.23}$$

The values of δ_l are determined by applying continuity equations at the border $r = a$ of the central potential. In the case of scattering by a rigid sphere of radius a, the phase shifts are given by (6.19) and (6.35):

$$\tan\delta_l = \frac{j_l(ka)}{n_l(ka)}, \qquad \lim_{ka\to 0}\tan\delta_l = \frac{(ka)^{2l+1}}{(2l+1)\big[(2l-1)!!\big]^2}. \tag{6.24}$$

If $ka = 0$, all the partial wave contributions vanish except for $l = 0$, due to the k^2 appearing in the denominator of the cross sections (6.22) and (6.23). We obtain

$$\sigma(\theta) = a^2, \qquad \sigma = 4\pi a^2. \tag{6.25}$$

The scattering is spherically symmetric and the total cross section is four times the area seen by classical particles in a head-on collision. This quantum result also appears in optics and is characteristic of long-wavelength scattering. The fact that σ is the total surface area of the sphere is interpreted by saying that the waves "feel" all this area.

Some features of scattering theory deserve to be stressed:

- The classical distance of closest approach to the z-axis of a particle with orbital angular momentum $\hbar l$ and energy E is l/k. Therefore, a classical particle is not scattered if $l > ka$. A similar feature appears in quantum mechanics, since the first and largest maximum of $j_l(kr)$ lies approximately at $r = l/k$. Thus, for $l > ka$, the maximum occurs where the potential vanishes: the largest value of l to be included is of order ka.
- The calculation of the probability current (4.18) with wave function (6.16) should yield interference terms in the whole space. They would be nonphysical consequences of assuming an infinite plane wave for the incident beam.

In practice, the beam is collimated and, as a consequence, the incident plane wave and the scattered wave are well separated, except in the forward direction (Fig. 6.2). On the other hand, in most experimental arrangements, the opening of the collimator is sufficiently large to ensure that there are no measurable effects of the uncertainty principle due to collimation (see Problem 12 of Chap. 2).

- Interference in the forward direction between the incident plane wave and the scattered wave gives rise to the important relation

$$\sigma = \frac{4\pi}{k}\mathrm{Im}\left[f_k(0)\right], \tag{6.26}$$

by comparing (6.21) and (6.23). The attenuation of the transmitted beam measured by $\mathrm{Im}\left[f_k(0)\right]$ is proportional to the total cross section σ. The validity of (6.26) (optical theorem) is very general and is not restricted to scattering theory.

- The previous description of a scattering experiment is made in the center of mass coordinate system. We must therefore use the projectile–target reduced mass and the energy for the relative motion to determine the value of k. Moreover, there is a geometrical transformation between the scattering angles θ and θ_{lab} because the two systems of reference move relative to each other with the velocity of the center of mass.

6.4* Solutions to the Coulomb and Oscillator Potentials

The hydrogen atom constitutes a two-body problem which can be transformed to a one-body form by changing to the center of mass frame. As a consequence, the reduced mass for relative motion should be used [as will be done in (8.22)]. However, for the sake of simplicity, we ignore the motion of the nucleus here, since it is much heavier than the electron.

It is always helpful to work with dimensionless variables, as in (4.22). In the case of the hydrogen atom, the natural length is the Bohr radius (Table A.1). Thus, one may use $u = Zr/a_0$. The solution to the radial equation (6.3) takes the form

$$R_{n_r l}(r) = N_{nl}(Z/na_0)^{3/2}\exp(-u/n)u^l L_{n_r}(u), \tag{6.27}$$

where $L_{n_r}(u)$ are polynomials of degree $n_r = 0, 1, 2, \ldots$ called Laguerre polynomials. The N_{nl} are normalization constants such that

$$\int_0^\infty r^2 R_{n_r l} R_{n'_r l}\mathrm{d}r = \delta_{n_r n'_r}. \tag{6.28}$$

The energy $Z^2|E_{\mathrm{H}}|/n^2$ is the ionization or binding energy, i.e. the amount of energy that must be given to the Z atom to separate an electron in the n state. Figure 6.3 represents the probability density as a function of the radial coordinate for the

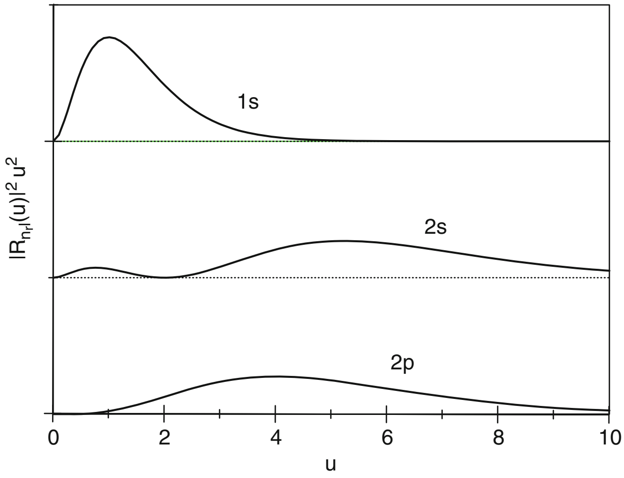

Fig. 6.3 Radial probability densities of the Coulomb potential

$n = 1, 2$ states (Table 6.2). The expression for the probability density includes a factor r^2 associated with the volume element (5.10).

Figure 6.4 combines the angular distribution associated with the spherical harmonics of Fig. 5.2 with the radial densities appearing in Fig. 6.3.

The Bohr radius a_0 may be compared with the expectation value of the coordinate r in the ground state of the hydrogen atom. According to Table 6.2, one gets

$$\begin{aligned} \langle 100|r|100\rangle &= \int_0^\infty \int_0^\pi \int_0^{2\pi} r^3 \, |\varphi_{100}|^2 \, \mathrm{d}r \sin\theta \mathrm{d}\theta \mathrm{d}\phi \\ &= \frac{4}{a_0^3} \int_0^\infty r^3 \exp(-2r/a_0) \mathrm{d}r = \frac{3}{2} a_0. \end{aligned} \tag{6.29}$$

There are also positive energy, unbound solutions to the Coulomb problem. They are used in the analysis of scattering experiments between charged particles.

In the harmonic oscillator, the dimensionless length is given by the ratio $u = r/x_\mathrm{c}$, as in (4.21). The radial eigenfunctions are

$$R_{n_r l} = N_{Nl} \frac{1}{\pi^{1/4} x_\mathrm{c}^{3/2}} \exp(-u^2/2) u^l F\left(-n_r, l + \frac{3}{2}, u^2\right). \tag{6.30}$$

The confluent hypergeometric function $F(-n_r, l + 3/2, u^2)$ is a polynomial of the order n_r in u^2 ($n_r = 0, 1, 2, \ldots$). Some radial probability densities are displayed in Fig. 6.5. The N_{Nl} are normalization constants such that (6.28) also holds true in this case. The energy eigenvalues are given by

Table 6.2 Radial dependence of the lowest solutions for the Coulomb potential and the three-dimensional harmonic oscillator

Coulomb potential				
n	n_r	l	N_{nl}	$L_{n_r}(u)$
1	0	0	2	1
2	1	0	2	$1-\frac{1}{2}u$
2	0	1	$1/\sqrt{3}$	1
3	2	0	2	$1-\frac{2}{3}u+\frac{2}{27}u^2$
3	1	1	$4\sqrt{2}/9$	$1-\frac{1}{6}u$
3	0	2	$4/27\sqrt{10}$	1
Three-dimensional harmonic oscillator				
N	n_r	l	N_{Nl}	$F\left(-n_r, l+\frac{3}{2}, u^2\right)$
0	0	0	2	1
1	0	1	$2\sqrt{2/3}$	1
2	1	0	$\sqrt{6}$	$1-\frac{2}{3}u^2$
2	0	2	$4/\sqrt{15}$	1
3	1	1	$2\sqrt{5/3}$	$1-\frac{2}{5}u^2$
3	0	3	$4\sqrt{2/105}$	1

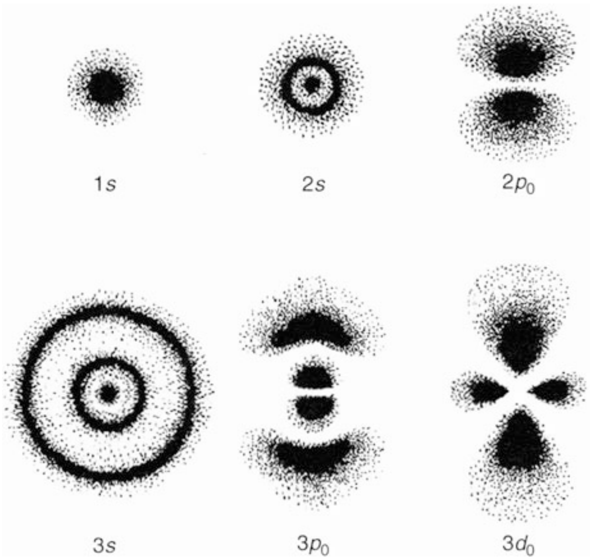

Fig. 6.4 Probability density plots of some hydrogen atomic orbitals. The density of the dots represents the probability of finding the electron in that region [41]. (Reproduced with permission from University Science Books)

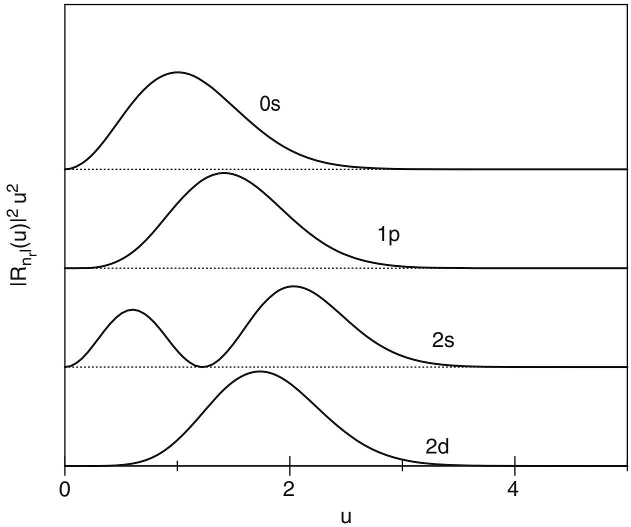

Fig. 6.5 Radial probability densities of the harmonic oscillator potential

$$E = \hbar\omega\left(N + \frac{3}{2}\right). \tag{6.31}$$

Using procedures similar to those applied for the linear harmonic oscillator, we may calculate the expectation values of the square of the radius and of the momentum. We thus verify the virial theorem (3.46) once again:

$$\langle N l m_l | r^2 | N l m_l \rangle / x_c^2 = \langle N l m_l | p^2 | N l m_l \rangle x_c^2 / \hbar^2 = N + \frac{3}{2}. \tag{6.32}$$

The lowest energy solutions are given on the right-hand side of Table 6.2.

Useful definite integrals are

$$\int_0^\infty u^n \exp(-au)\mathrm{d}u = \frac{n!}{a^{n+1}}, \qquad \int_0^\infty u^{2n} \exp(-u^2)\mathrm{d}u = \frac{(2n-1)!!\sqrt{\pi}}{2^{n+1}},$$

$$\int_0^\infty u^{2n+1} \exp(-u^2)\mathrm{d}u = \frac{n!}{2}.$$

6.5* Some Properties of Spherical Bessel Functions

The spherical Bessel functions $j_l(kr)$ [and the Neumann $n_l(kr)$] satisfy the differential equation

Table 6.3 Lowest spherical Bessel functions

l	j_l	n_l
0	$\frac{1}{\rho}\sin\rho$	$-\frac{1}{\rho}\cos\rho$
1	$\frac{1}{\rho^2}\sin\rho - \frac{1}{\rho}\cos\rho$	$-\frac{1}{\rho^2}\cos\rho - \frac{1}{\rho}\sin\rho$
2	$\left(\frac{3}{\rho^3} - \frac{1}{\rho}\right)\sin\rho - \frac{3}{\rho^2}\cos\rho$	$-\left(\frac{3}{\rho^3} - \frac{1}{\rho}\right)\cos\rho - \frac{3}{\rho^2}\sin\rho$

$$-\frac{\hbar^2}{2M}\left[\frac{\mathrm{d}^2}{\mathrm{d}r^2} + \frac{2}{r}\frac{\mathrm{d}}{\mathrm{d}r} - \frac{l(l+1)}{r^2}\right] j_l(kr) = \frac{\hbar^2 k^2}{2M} j_l(kr). \tag{6.33}$$

Their asymptotic properties for large arguments are

$$\lim_{\rho\to\infty} j_l(\rho) = \frac{1}{\rho}\sin\left(\rho - \frac{1}{2}l\pi\right), \qquad \lim_{\rho\to\infty} n_l(\rho) = -\frac{1}{\rho}\cos\left(\rho - \frac{1}{2}l\pi\right), \tag{6.34}$$

while for small arguments they are

$$\lim_{\rho\to 0} j_l(\rho) = \frac{\rho^l}{(2l+1)!!}, \qquad \lim_{\rho\to 0} n_l(\rho) = -\frac{(2l-1)!!}{\rho^{l+1}}. \tag{6.35}$$

The spherical Hankel functions are defined by

$$h_l^{(+)}(\rho) = j_l(\rho) + \mathrm{i}n_l(\rho), \qquad h_l^{(-)}(\rho) = j_l(\rho) - \mathrm{i}n_l(\rho). \tag{6.36}$$

Due to (6.34), these have the asymptotic expressions

$$\lim_{\rho\to\infty} h_l^{(+)}(\rho) = \frac{(-\mathrm{i})^{l+1}}{\rho}\exp(\mathrm{i}\rho), \qquad \lim_{\rho\to\infty} h_l^{(-)}(\rho) = \frac{(\mathrm{i})^{l+1}}{\rho}\exp(-\mathrm{i}\rho). \tag{6.37}$$

The first three j_ls and n_ls are given in Table 6.3.

Problems

Problem 1. Calculate the difference in the excitation energy of $n = 2$ states between hydrogen and deuterium atoms. Hint: use the reduced mass instead of the electron mass.

Problem 2. 1. Assign the quantum numbers nlj to the eigenstates of the Coulomb problem with $n \leq 3$.
2. Do the same for the three-dimensional harmonic oscillator with $N \leq 3$.

Problem 3. 1. Obtain the degeneracy of a harmonic oscillator shell N, including the spin.

2. Obtain the average value $\langle|L^2|\rangle_N$ of the operator $\hat{L}^2$ in an N shell.
3. Calculate the eigenvalues of a harmonic oscillator potential plus the interaction [see (7.16)]

$$-\frac{\omega}{16}\left(\frac{1}{\hbar}\hat{L}^2 - \hbar N(N+3)\right) - \frac{\omega}{4\hbar}\hat{\boldsymbol{L}}\cdot\hat{\boldsymbol{S}},$$

for $N = 0, 1, 2, 3$.
4. Give the quantum numbers of the states with minimum energy for a given shell N.

Problem 4. 1. Find the energy and the wave function for a particle moving in an infinite spherical well of radius a with $l = 0$. Hint: replace $\Psi(r) \to f(r)/r$.

2. Solve the same problem using the Bessel functions given in Sect. 6.5**.

Problem 5. 1. Find the values of r at which the probability density is at a maximum, assuming the $n = 2$ states of a hydrogen atom.

2. Calculate the mean value of the radius for the same states.

Problem 6. Solve the harmonic oscillator problem in Cartesian coordinates. Calculate the degeneracies and compare them with those listed in Table 6.1.

Problem 7. 1. Find the ratio between the nuclear radius and the average electron radius in the $n = 1$ state, for H and for Pb. Use $R_{\text{nucleus}} \approx 1.2A^{1/3}$ F, $A(\text{H}) = Z(\text{H}) = 1$, $A(\text{Pb}) = 208$ and $Z(\text{Pb}) = 82$.

2. Do the same for a muon ($M_{\mu} = 207M_{\text{e}}$).
3. Is the picture of a pointlike nucleus reasonable in all these cases?

Problem 8. Replace $r^2 \to s$ in the radial equation of a harmonic oscillator potential. Find the changes in the constants $l(l+1)$, $M\omega^2$ and E that yield the Coulomb radial equation. Hint: make the replacement $R(r) \to s^{1/4}\Phi(s)$ and construct the radial equation using $s \equiv r^2$ as variable.

Problem 9. The positronium is a bound system of an electron and a positron (the same particle as an electron but with a positive charge). Their spin–spin interaction energy may be written as $\hat{H} = a\hat{\boldsymbol{S}}_{\text{e}}\cdot\hat{\boldsymbol{S}}_{\text{p}}$, where e and p denote the electron and positron, respectively.

1. Obtain the energies of the resultant eigenstates (see Problem 11 of Chap. 5).
2. Generalize (6.15) to the product of two arbitrary angular momentum $\hat{\boldsymbol{J}}_1 \cdot \hat{\boldsymbol{J}}_2$

Problem 10. Calculate the splitting between the $2p$ states with $m = 1/2$ of a hydrogen atom in the presence of spin–orbit coupling and a magnetic field $\boldsymbol{B}$ in the z-direction:

1. At the limit $v_{\text{so}} = 0$
2. At the limit $B_z = 0$
3. As a function of the ratio $q = 2\mu_{\text{B}}B_z/\hbar^2 v_{\text{so}}$

Problem 11. Calculate the current associated with the spherical wave $A\exp(\mathrm{i}kr)/r$ and show that the flux within a solid angle $\mathrm{d}\Omega$ is constant.

Problem 12. A beam of particles is being scattered from a constant potential well of radius a and depth V_0. Calculate the differential and the total cross section in the limit of low energies.
Hint: Consider only the $l = 0$ partial waves.

1. Obtain the interior logarithmic derivative (times a) for $r = a$ (see Problem 4).
2. Obtain the exterior logarithmic derivative (times a) for $r = a$ in the low energy limit.
3. Calculate $\tan\delta_0$.
4. Calculate $\sigma(\theta)$.
5. Calculate σ.

Problem 13. Consider a planar motion.

1. What is the analogue of spherical symmetry in a two-dimensional space? Find the corresponding coordinates.
2. Write down the operator for the kinetic energy in these coordinates and find the degeneracy inherent in potentials with cylindrical symmetry.
3. Find the energies and degeneracies of the two-dimensional harmonic oscillator problem.
4. Verify that the function

$$\varphi_n = \frac{1}{x_\mathrm{c}\sqrt{\pi n!}}\exp(-u^2/2)u^n\exp(\pm\mathrm{i}n\phi)$$

   is an eigenstate of the Hamiltonian ($u = \rho/x_\mathrm{c}$).

Problem 14. Consider the outer electron of a Rydberg atom

1. Calculate the quantum frequency ω_{ph} of the photon emitted in the transition $\varphi_{n,n-1,n-1} \rightarrow \varphi_{n-1,n-2,n-2}$ and the classical frequency ω_{cl} of the rotational motion of the electron.
2. Which principle relates these two frequencies?